



High energy milling activation time dependence of the mass loss during phase thermal decomposition of quartz, calcite and apatite

Зависимост на масовите загуби от времето на интензивно енергетично смилане при термично разлагане на кварц, калцит и апатит

Bilyana Kostova¹, Vilma Petkova², Ventseslav Stoyanov³
Биляна Костова¹, Вилма Петкова², Венцеслав Стоянов³

¹ New Bulgarian University, Department of Natural Sciences, 21 Montevideo Blvd., 1618 Sofia, Bulgaria;
E-mail: bkostova@nbu.bg

² Institute of Mineralogy and Crystallography, Bulgarian Academy of Sciences, Acad. G. Bonchev Str., Bl. 107, 1113 Sofia, Bulgaria; E-mail: vilmapetkova@gmail.com

³ University of Structural Engineering and Architecture „Lyuben Karavelov“, 175 Suhodolska Str., 1373 Sofia, Bulgaria;
E-mail: vensy.stoyanov@gmail.com

Keywords: CaO-SiO₂-P₂O₅ cement system, thermal analysis, ancient cement.

Introduction

The natural mineral mixture of apatite, quartz, and calcite is investigated system as a raw material for fertilizers and soil improvers (Kawatra, Carlson, 2014). The predominant components in chemical composition of the mixture, CaO, SiO₂, and P₂O₅, are essential part of ancient and modern cement and ceramic composites. They are successfully investigated by thermal analysis. On the other hand, their preparation includes preliminary milling of the raw material. Consequently, the study of their behavior after milling by thermal analysis is of practical importance for modern cement and ceramic composites and archaeological chemistry as well.

It is well known that milling and rising temperatures lead the formation of defects in minerals. The defectiveness in studied system will occur in the apatite, mainly by redistribution of CaO and P₂O₅ (Chaikina, 2002).

The aim of this work is to reveal the dependencies between the milling time and the cationic/anionic substitution at elevating temperatures, presented by experimentally measured mass losses.

Materials and methods

The investigated raw material is from Sanadinovo, Bulgaria. It is low-phosphate and unpromising ore (Sample B0) (Kovatchev et al., 1991), having the following chemical composition (mass%): 38.97 SiO₂, 26.34 CaO, 14.61 P₂O_{5tot}, 7.91 R₂O₃ (R₂O₃ = Fe₂O₃+Al₂O₃) 2.63 F₂, 2.10 K₂O, 1.13 Na₂O, 0.95

SO_x, 0.84 MgO, and the mineral composition: – quartz, calcite and fluorapatite.

The raw sample B0 was high energy milled (HEM) 10, 30, 60, 120, and 240 min (samples B10, B30, B60, B120, and B240, respectively) in a planetary mill Pulverisette-5, Fritsch Co (Germany), with a diameter of the Cr-Ni milling bodies of 20 mm, and sample mass of 0.020 kg.

Thermal analyses (TG-DTG) were performed on a LABSYS/SETSYS evo thermal analyzer (SETARAM, France) in air medium in the temperature range – from room temperature (RT) to 1050 °C and heating rate of 10 °C.min⁻¹.

Results and discussion

The measured mass losses (ML) of HEM activated samples are separated in three temperature intervals: 50–370 °C (0.40–2.70% ML); 430–530 °C (0.72–1.67% ML) and 530–920 °C (decrease from 6.40% to 4.56% ML). ML increase in the first temperature interval, while in the third ML decrease from 6.40% to 4.65%. In the second temperature range the mass losses increase from 0.95% to 1.67% (B120) and decrease to 0.92% (B240) (Fig. 1a). In the 1st temperature range, the process of dehydration occurs. After application of HEM, the free surface of the sample increases and it easily incorporates water from the atmosphere. This water is released during the process of dehydration (Chaikina, 2002). In the 2nd range, the dehydroxylation (release of structurally bound water) and the decarbonation (release

of CO_2) take place. The dehydroxylation is probably from HCO_3^- and $\text{H}_2\text{P}_2\text{O}_7^{2-}$, formed during the HEM activation, as the presence of structurally bound water is explained by the charge compensation mechanism in isomorphous substitutions (Chaikina, 2002). At the beginning of the 3rd range the decarbonation occurs simultaneously with dehydroxylation, and the CO_3^{2-} release from OH^- positions in apatite (A-type isomorphism) occurs – 530–580 °C. During the 3rd temperature range, the other three stages of decomposition are distinguished: (i) decarbonation of CO_3^{2-} in apatite, realized by isomorphous substitution of PO_4^{3-} by CO_3^{2-} (B type isomorphism) – 670–710 °C; (ii) decarbonation of CO_3^{2-} from calcite – 750–850 °C; and (iii) decarbonation of CO_3^{2-} from apatite, realized by isomorphous substitution of PO_4^{3-} by CO_3^{2-} and occupancy of the vacancy (A-B type isomorphism) – 800–840 °C, (Elliott, 1994; Chaikina, 2002; Petkova et al., 2015) (Fig. 1a).

Based on measured ML in the three decomposition temperature intervals and time of HEM activation,

the dependencies with a coefficient of determination above 0.9 were made (Fig. 1b–d). The obtained dependencies allow commenting on the relationship between ML changes and HEM activation time.

Figure 1b shows the exponential dependence of HEM activation time by ML for apatite decarbonation of CO_3^{2-} from OH-position (A-type isomorphism) with the best fit: $y = \exp(0.167 - 0.011x - 4.792 \cdot 10^{-5}x^2)$ ($R^2 = 0.94$). The measured increase of ML from 0.95% to 1.82% is due to increase of CO_3^{2-} incorporation in OH-positions, i.e. structural defects rise. It is likely that A-type defects formation is related to CO_2 absorption from the air (Koleva et al., 2012). The decrease in ML after 120 min HEM should be explained by both of the particles' aggregation and the difficult access of CO_2 to the fresh surface, where the reaction occurs.

Figure 1c presents exponential decrease of ML with increase the HEM activation time for CO_3^{2-} decarbonation from PO_4^{3-} position (B-type isomor-

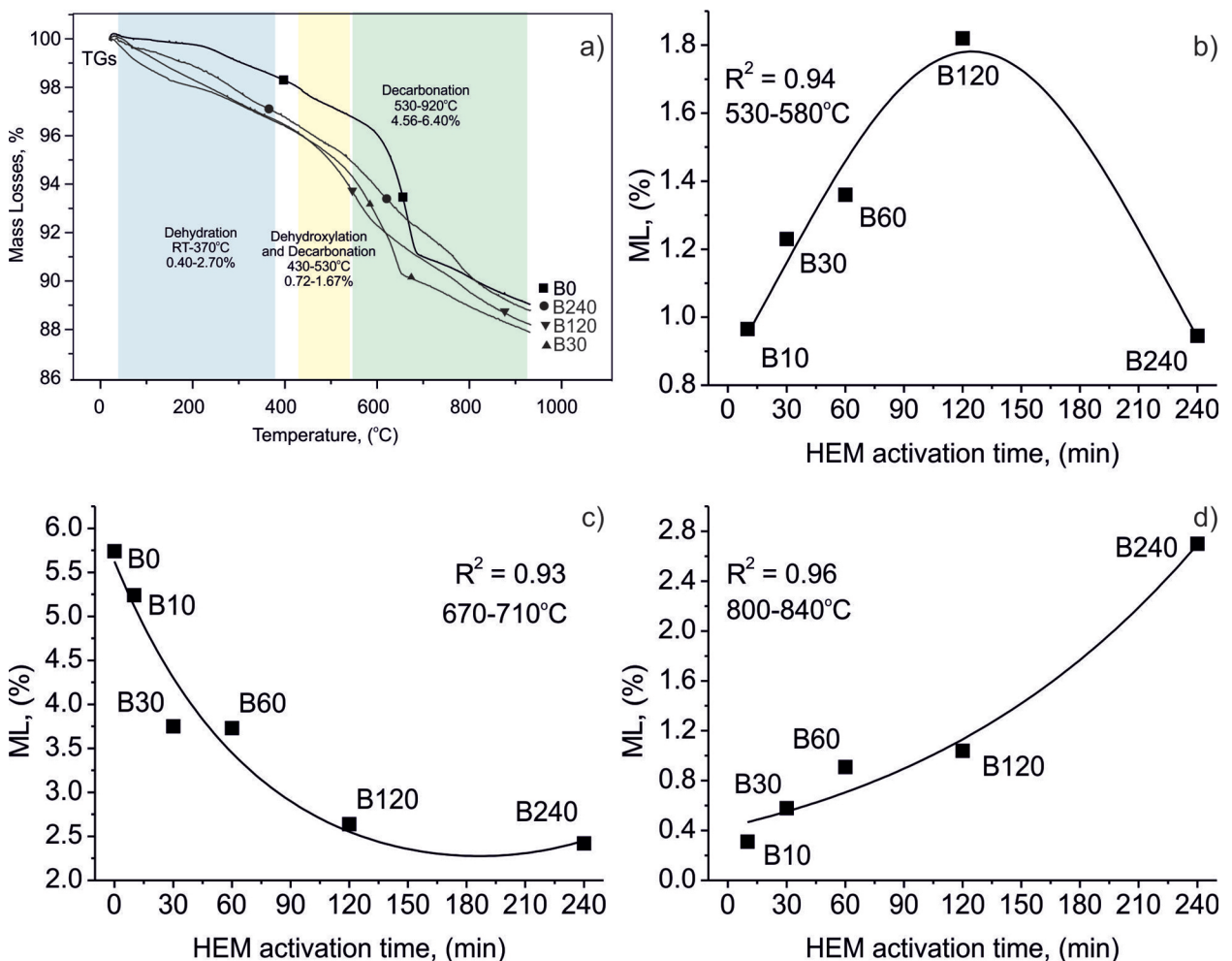


Fig. 1. a, TGs curves of B0, B30, B120, and B240; HEM activation time dependence of the measured ML during decarbonation and best fit to these data: b, apatite A-type substitution; c, apatite B-type substitution; d, apatite A-B-type substitution

phism) with the best fit: $y = \exp(1.727 - 0.009x + 2.600 \cdot 10^{-5}x^2)$ ($R^2 = 0.93$) in the temperature range 670–710 °C. The reduction of ML from B0 (5.74%) to B240 (2.42%) is by 58%, which shows a significant decrease in CO_3^{2-} at B-type position in apatite.

Figure 1d presents exponential increase of ML with increase the HEM activation time for CO_3^{2-} decarbonation from PO_4^{3-} position and vacancy (A-B-type isomorphism) (Lafon et al., 2008; Tonsuaadu et al., 2012), with the best fit: $y = \exp(-0.747 - 0.008x - 0.355x^2)$ ($R^2 = 0.96$). The ML rise from 0.31% (B0) to 2.70% (B240), i.e., with 88%. This is a result of defects increasing during HEM activation.

The quartz from the studied system stay inactive during HEM activation (does not participate in isomorphic processes), due to high hardness.

Conclusion

A relationship has been established between mass losses (ML) and high energy milled (HEM) time. It can be used to determine the tendency for presence/absence of defects in the apatite structure. In well-studied systems, such as the current one, the thermal method is sufficiently sensitive and can justify the need for structural studies.

Acknowledgements: This work was supported by the Bulgarian Science Research Found (grant number KP-06-N39/9 – B. K., V.S).

References

- Chaikina, M. V. 2002. *Mechanochemistry of Natural and Synthetic Apatites*. Novosibirsk, Publishing House of SB RAS, Branch “GEO”, 219 p. (in Russian).
- Elliott, J. C. 1994. *Structure and Chemistry of the Apatite and Other Calcium Orthophosphate, Studies in Inorganic Chemistry*. Amsterdam, Elsevier, 389 p.
- Kawatra, S. K., J. T. Carlson. 2014. *Beneficiation of Phosphate Ore*. Society for Mining, Metallurgy & Exploration. USA, Colorado, Englewood, 153 p.
- Koleva, V., V. Petkova. 2012. IR spectroscopic study of high energy activated Tunisian phosphorite. – *Vib. Spectrosc.*, 58–125.
- Kovatchev, V., S. Strashimirov, P. Petrov. 1991. *Non-metallic Ores*. Sofia, University of Mining and Geology, 268 p. (in Bulgarian).
- Lafon, J. P., E. Champion, D. Bernache-Assollant. 2008. Processing of AB-type carbonated hydroxyapatite $\text{Ca}_{10-x}(\text{PO}_4)_{6-x}(\text{CO}_3)_x(\text{OH})_{2-x-2y}(\text{CO}_3)_y$ ceramics with controlled composition. – *J. Europ. Ceram. Soc.*, 28, 1–139.
- Petkova, V., V. Koleva, B. Kostova, S. Sarov. 2015. Structural and thermal transformations on high energy milling of natural apatite. – *J. Therm. Anal. Calorim.*, 121, 1, 217–225.
- Tonsuaadu, K., K. A. Gross, L. Plüduma, M. Veiderma. 2012. A review on the thermal stability of calcium apatites. – *J. Therm. Anal. Calorim.*, 110, 2, 647–659.